RSC Advances

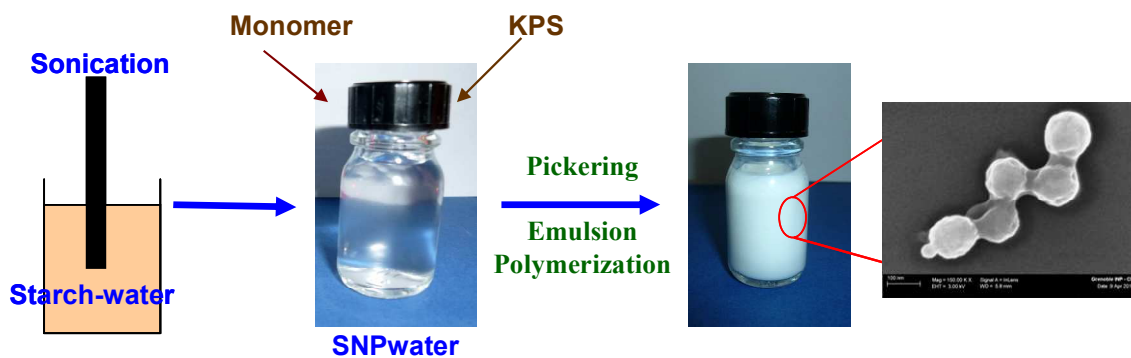# Starch Nanoparticles produced via ultrasonication as a sustainable stabilizer in Pickering Emulsion polymerization

SCHOLARONE™
Manuscripts

Table of content

A facile and effective method for the Pickering emulsion polymerization of acrylate monomer was reported, using SNPs as a sole stabilizer. The SNPs were produced via ultrasonication in water without any chemical additives

1   **Starch nanoparticles produced via ultrasonication as a sustainable stabilizer in**

2   **Pickering emulsion polymerization**

3

4

5

6

7   **Sihem Bel Haaj[a], Albert Magnin[b], Sami Boufi*[a]**

8

9   *[a] University of Sfax- Sfax Faculty of Science-LMSE BP 802-3018 Sfax, Tunisia[bb] Laboratoire*

10   *Rhéologie et Procédés, Univ. Grenoble Alpes, LRP, F-38000 Grenoble, France*

11   *CNRS, LRP, F-38000 Grenoble, France*

12

13   **Corresponding author at:** *Faculty of Science* -LMSE-University of Sfax BP 1171 3000-
14   Sfax-Tunisia

15   *** Tel: 216 47274400**

16   *** Fax: 216 74274437**

17   *** e-mail address:** sami.boufi@fss.rnu.tn

18   *e-mail: sami.boufi@fss.rnu.tn

19

20

21

22   **Abstract**

23

24   Pickering emulsion polymerizations using starch nanoparticles (SNPs) as a sole stabilizer and

25   persulfate as an initiator have been successfully accomplished. The SNPs were prepared in

26   water via high-power ultrasonication without the addition of any chemical reagent. The

27   polymer dispersion stabilized by SNPs proved to be stable for several months, when the SNP

28   content was above 4 wt% relative to the monomer phase. As the SNP loading increased, the

29   particle sizes of the polymer dispersion decreased steadily, confirming the key role of the

30   SNPs in the stabilization process. On the basis of the zeta-potential measurement and change

31   in polymer particle size during emulsion polymerization, a mechanistic aspect of the

32   Pickering emulsion polymerization is proposed. The film-formation properties of the

33   nanocomposite dispersion and the optical properties of the ensuing films are also discussed. It

34   was shown that nanocomposites formed prepared via the Pickering emulsions route displayed

35   better optical transparency than that obtained by ex-situ mixing route.

36

37   *Key words*: Pickering, starch nanoparticles, emulsion polymerization.

38

39 **Introduction**

40

41 In recent years, the production of nanoparticles from naturally occurring biopolymers such as

42 cellulose[1], chitin[2] and starch[3] has drawn considerable attention because they combine the

43 advantageous properties of biopolymers, namely the broad range of chemical modifications,

44 renewability and sustainability, with the specific attributes of nanosized materials, which in

45 turn has expanded the spectrum of potential applications.

46 Although much less studied than nanocellulose or cellulose nanocrystals, the extraction and

47 uses of starch nanoparticles (SNP) have been the subject of numerous reports[4,5]. Current

48 potential use of SNP is as a reinforcing phase in a polymeric matrix to improve the

49 mechanical and barrier properties of the materials[6]. SNP can be produced via the acid

50 hydrolysis route, leading to starch nanocrystals with a well defined platelet-like shape and a

51 highly crystalline structure. It can be also produced via a physical disintegration process

52 without the need to implement any chemical treatment or to add any chemical reagent. This

53 latter route affords environmentally friendly approaches and is arousing increasing interest. In

54 this context, we have described an efficient approach for the preparation of nano-sized starch

55 particles using the purely physical method of high-intensity ultrasonication[7]. The process is

56 based on the high-power ultrasonication of a suspension of starch granules in water at 1 to 2%

57 consistency and at a temperature of 8-10°C. It was shown that complete conversion of the

58 starch granules from a micronic to a nanometric scale is achieved after 75 min ultrasonication,

59 generating nanoparticles from 20 to 100 nm in size. This process constitutes a green approach

60 to the production of SNP with a high yield and without the need to undertake any post

61 purification treatment.

62 Currently, SNPs are mainly used as a nanofiller in polymer matrixes, where an improvement

63 in the barrier properties and mechanical properties has been reported[8]. In most processing

64 routes for preparing SNP-based nanocomposite, two-pot mixing involving an SNP suspension

65 with waterborne polymer dispersion remained the most commonly used and most efficient

66 approach, ensuring the preservation of the individualized state of the nanoparticles. However,

67 this approach is time-consuming and involves multiple steps.

68 *In situ* polymerization in the presence of SNPs could be envisaged as an alternative way to

69 produce a one-pot nanocomposite dispersion ready for use and with good dispersion of the

70 nanofiller within the matrix. Preparation of the emulsion with the nanoparticles present (*in-*

71 *situ* approach) has the further advantage of: (i) creating the formulation in one step rather than

72 through the so-called *ex-situ* approach requiring the nanoparticles to be blended with the

73 polymer latex after polymerization has taken place, (ii) reducing the necessary processing

74 steps, and (iii) avoiding the dilution and mixing phase. In addition, this strategy results in a

75 more efficient binding of the nanoparticles onto the polymer particles. This allows improved

76 tailoring of the nanocomposite characteristics on the nanoscale level, favoring nanoparticle

77 individualization[9].

78 The presence of nanoparticles during emulsion polymerization might be further exploited to

79 induce what is known as Pickering stabilization. Using solid particles, conventional

80 emulsifying agents can be omitted and hazardous surfactants may be replaced by less harmful

81 materials and more environmentally-friendly components[10]. The use of surfactants is known

82 to have an adverse effect on the mechanical and water-resistance properties of the resulting

83 films[11], and also contribute to generating foams and fine bubbles. All of these attributes make

84 the Pickering polymerization approach of great interest.

85 In Pickering emulsions, solid particles of intermediate wettability with dimensions ranging

86 from several nanometers to several micrometers attach to liquid-liquid interfaces and provide

87 emulsion stability. Emulsions stabilized by solid particle emulsions are known to display

88 higher stability against coalescence compared to systems stabilized by surfactants. The

89   stabilization has been explained by the volume exclusion created by the adsorbed particles

90   preventing contact between neighboring oil–water interfaces and by the Gibbs free energy

91   penalty incurred by removing the adsorbed solid particles away from the interface[12].

92   The use of polysaccharide-based nanoparticles, such as cellulose nanofibrils[13], cellulose

93   nanocrystals[14] and, recently, starch nanocrystals[15] and cellulose as solid-emulsifiers has

94   received increasing attention in a broad field of applications such as food technology,

95   cosmetic formulation, and pharmaceutical products. The wide availability of these particles,

96   their relative ease of production, combined with their biodegradability and non-toxic

97   character, are all factors driving the use of this class of nanoparticle as a stabilizer to replace

98   synthetic surfactant.

99   The use of SNPs as a Pickering stabilizer for the *in situ* emulsion polymerization to elaborate

100   SNP-based nanocomposite has not yet been explored. In a recent work, starch nanoplatelets

101   were found to provide a synergistic effect with cationic surfactant in stabilizing butyl

102   methacrylate mini-emulsions during polymerization[16]. The emulsion polymerization strategy

103   using SNPs as a stabilizing agent is expected to result in better attachment of the

104   nanoparticles onto the polymer particles, which in turn would lead to improved tailoring of

105   the nanocomposite characteristics on the nanoscale level and favor nanoparticle

106   individualization[17], and possibly even promote the formation of chemical linkages between

107   the polymer and the nanofiller. This, in turn, is expected to lead to higher film transparency,[18]

108   with a higher nanoparticle reinforcing potential. The use of water as a dispersion medium also

109   has environmental benefits and gives a direct one-pot route to waterborne film-forming

110   nanocomposite dispersions ready for use as water-based coatings and adhesives.

111   In this research, we report the successful Pickering emulsion polymerization of acrylic

112   monomers using SNPs prepared via ultrasonication as a sole stabilizer. The effect of the SNP

113   content on the particle size, the colloidal properties of the polymer dispersion and the optical

114   properties of the ensuing nanocomposites were investigated.

115   **Experimental set-up**

116   *Materials*

117   Butyl methacrylate (BMA, Aldrich, 99 wt%) was distilled under vacuum and kept refrigerated

118   until use. Potassium persulfate (KPS) was supplied by Sigma Aldrich and used without

119   further purification. Distilled water was used for all the polymerization and treatment

120   processes. Waxy maize (WaxylisTM, > 99% amylopectin) was provided by Roquette S.A.

121   (Lesterm, France).

122   *Starch nanoparticle preparation*

123   The SNPs were prepared by adopting the procedure described in our previous work[7]. More

124   specifically, 1.5 g of starch was added to 100 ml of water and sonicated at 80% power output

125   for 75 min using a 20kHz Branson digital Sonifier S-450D (Germany) coupled with a horn

126   with a tip diameter of 13 mm. The ultrasonication treatment was conducted at a temperature

127   below 10°C. The temperature was reached by immersing the starch suspension in a

128   thermostated bath maintained at a temperature of 8 ± 1°C. At the end of the ultrasonication

129   treatment, the starch suspension turned from turbid white to transparent.

130   *Emulsion polymerization*

131   The emulsion polymerization of BMA was carried out in the presence of SNP suspension at

132   70°C using KPS as an initiator. The typical formulation is the following: Water (17 g),

133   monomers MBA (3g) and KPS (0.12 g) and SNPs (from 0.05 up to 0.3 g).

134   The following procedure was adopted to implement the emulsion polymerization reaction: the

135   appropriate amount of SNPs in water (with a solid content of 2%) was weighed first, then

136   BMA monomer and KPS initiator were added and kept under magnetic stirring for several

137   minutes to create the monomer emulsion. The resulting emulsion was then flushed with N_2

138   and the polymerization started by heating the emulsion to 70°C. Polymerization occurred

139   within 3h.

Particle size determination

141   The emulsion droplet diameters were measured at 25°C using a Malvern Nano-Zetasizer ZS

142   instrument at a fixed scattering angle of 173°. The dispersion was diluted to about 5 wt% with

143   distilled water before starting the measurements. The cumulative average determined from the

144   dynamic light scattering (DLS) correlation curve was fitted with a single exponential decay to

145   determine the particle size distribution. Each measurement was performed in triplicate and the

146   values obtained averaged to obtain the mean particle size.

Zeta-Potential Measurement

148   The zeta-potentials were measured at 25°C using a laser Doppler electrophoresis apparatus

149   (Malvern Nano-Zetasizer ZS, UK). The sample consistency in water was set at 0.01% (w/v).

150   The measurements were performed three times for each sample.

FE-SEM microscopy

152   Field Emission Scanning Electron Microscope (FE-SEM) images were obtained with a Zeiss

153   Supra40. Images were created by the SMARTSEM software. A drop of a diluted suspension

154   of starch (with a solid content of about 0.02wt.%) was deposited on a silicon wafer,

155   evaporated at room temperature and then coated with a thin carbon layer limited to 3 nm

156   applied by sputtering. In the case of the polymer dispersion, the drop of diluted dispersion

157   (0.01%) was deposited on a silicon wafer and freeze-dried to prevent the polymer particles

158   from coalescing.

Dynamic mechanical analysis (DMA)

160   Dynamic mechanical analysis (DMA) experiments were conducted in tension mode using a

161   PYRIS Diamond DMA (Perkin- Elmer, Waltham, MA, USA). Temperature scans were run

162   from -50°C to 100°C at a heating rate of 2°C min-1, a frequency of 1 Hz and an amplitude of

163 10 μm. The storage (E′) as well as the loss factor tan δ were measured as a function of

164 temperature. Sample dimensions were about 20mm (length), 5 mm (width) and 0.1– 0.3 mm

165 (thickness).

166 The nanocomposite films were prepared via casting of the nanocomposite dispersion in a

167 Teflon mold and storing 40°C until water evaporation was completed.

168 **Results and discussion**

169 *SNP properties*

170 The nano-sized starch particles were prepared via high-intensity ultrasonication without any

171 chemical additives. The process is based on the high-power ultrasonication of a suspension of

172 starch granules in water at 2% consistency for 75 min at a temperature of 8-10°C. After

173 ultrasonication, the suspension became transparent without any change in the fluidity of the

174 solution, which is a good indication of the small size of the starch nanoparticles. This is

175 further confirmed from the Tyndall scattering effect when the suspension is illuminated by a

176 laser beam (see inset Figure 1). It is worth noting that the optical appearance of the dispersion

177 did not change with time and no trace of settling was noted after storing over a period

178 exceeding one month at 8-10°C. This physical method for producing fine starch NPs

179 involving ultrasonication without any chemical additive has been recently developed in our

180 group and has proved to be efficient in reducing the size of starch granules from the micronic

181 to the nanometric scale.   The particle size distribution determined from DLS showed a

182 monomodal narrow distribution centered at 37 nm. FE-SEM observation of the particles after

183 depositing a drop of diluted suspension of NPS and drying at room temperature showed

184 nanosized particles 35 to 50 nm in size (Figure 2). The apparent tendency of the nanoparticles

185 to self-associate is inherent to their chemical structure (i.e. high density of surface hydroxyl

186 groups), their nanosized scale and the mode of sample preparation (water evaporation at room

187 temperature). Although it is hard to have a clear-cut indication about the exact morphology of

188   the SNPs, the FE-SEM observation revealed the presence of both a granular, as well as a

189   platelet-like shape. The zeta-potential of the SNP from waxy maize was - -3 mV over a pH

190   ranging from 4 to 9, which indicates that the SNPs did not hold any surface charge. The

191   reason for choosing waxy starch lies in its high amylopectin content and the quasi absence of

192   amylose in the starch backbone, which is likely to leach out from the SNPs. Another reason is

193   the insensitivity of SNPs to water, even after prolonged heating at 70°C. Actually, as shown

194   in Figure 3, the particle size remained unchanged at around 37 nm when the SNP suspension

195   was heated for more than 4h at 70°C. This aspect is essential for the following work, in which

196   SNPs were used as a Pickering stabilizer in the emulsion polymerization of acrylic monomer.
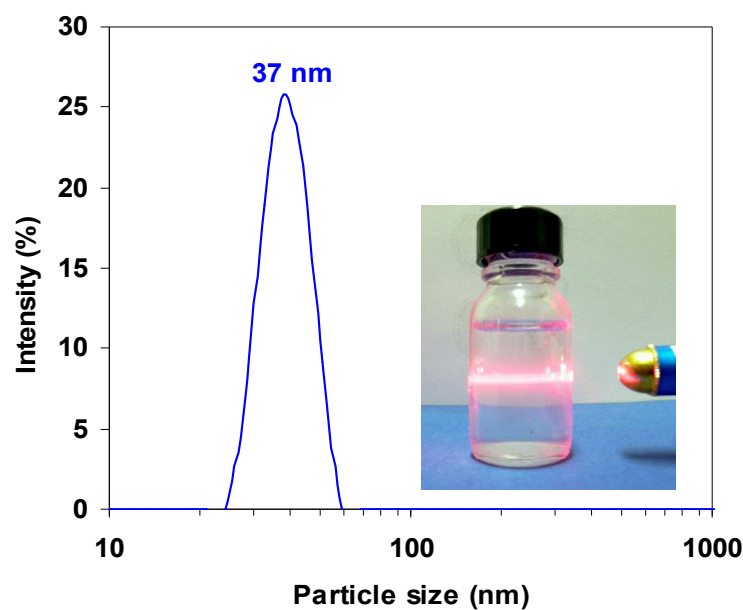
197

198   **Figure 1: Particle size distribution of SNP from waxy maize and the appearance of the**

199   **SNP suspension (at 1.5 wt.% solid content). Photo showing the Tyndall scattering effect**

200   **(He–Ne laser, 632.8 nm) confirming the presence of colloidal SNPs.**
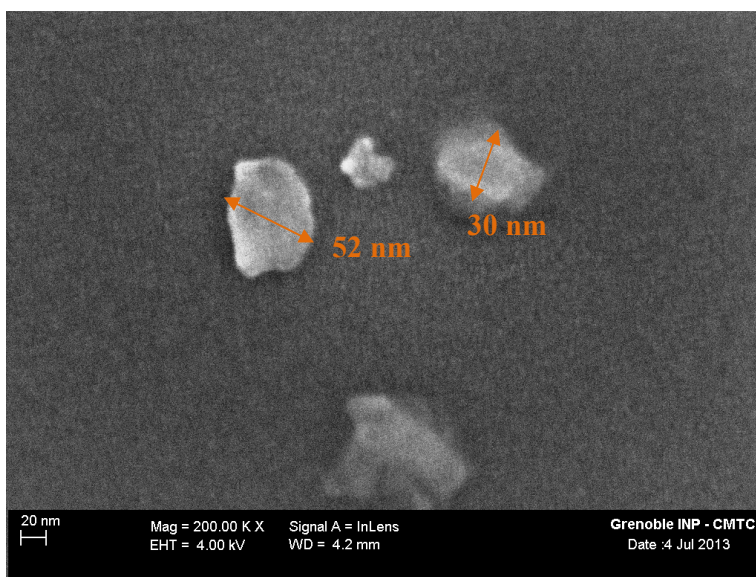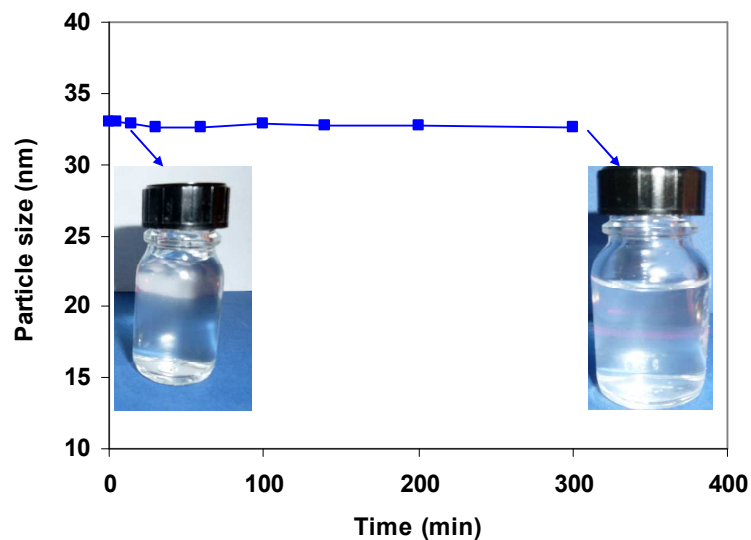
201

202

203
204
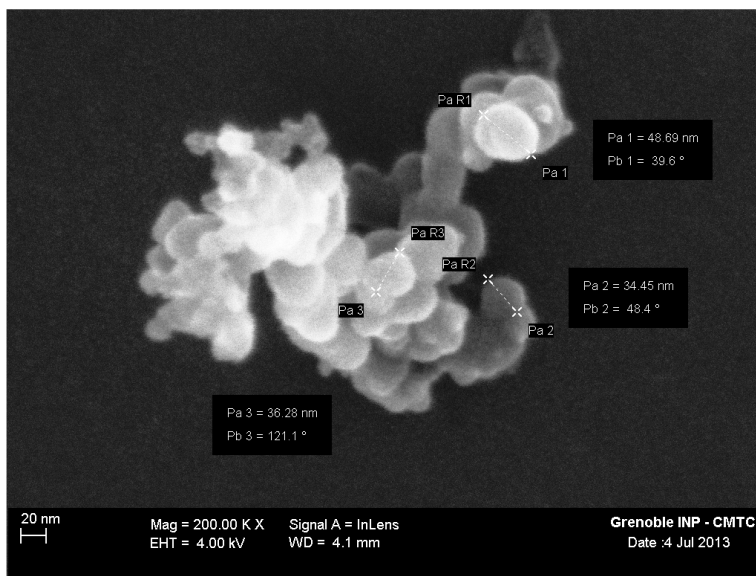
205
206

207
208
209

210   **Figure 2: FE-SEM images of SNPs from waxy maize used in the present work.**

211

212

Figure 3: Particle size change in SNPs vs time as the suspension with 2% solid content was exposed to a temperature of 70°C.

213
214
215

216 To determine the water contact angle on the SNPs, a thin transparent film was formed on a

217 glass slide. The film was prepared by depositing drops of the SNP suspension containing 10%

218 of isopropanol to improve the complete wetting of the glass. A thin, transparent and

219 homogenous film was obtained after drying at 50°C for several hours. This approach has been

220 proven to be effective in determining the water contact angle of SNP, giving a constant angle

221 around 43° (Figure 4).

222
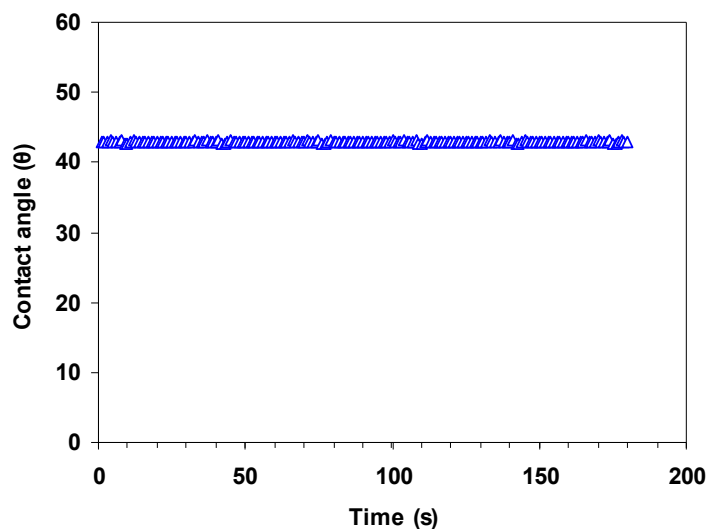
Figure 4. Water contact angle changes vs. time of SNPs from waxy maize films deposited on a glass slide.

225

226 *Pickering emulsion polymerization*

227

228 The first experiment run in the emulsion polymerization of BMA was carried out in the

229 presence of 6% SNP as sole stabilizer. It was conducted by adding the initiator to the mixture

230 of BMA and the aqueous suspension of SNP, followed by heating at 70°C. Progressively, the

231 dispersion turned from a translucent to a white emulsion with increasing polymerization,

232 giving stable polymer latex free from any coagulum after 3h of reaction at 70°C. A

233 monomodal size distribution centered at 195 nm was obtained and the polymer dispersion

234 remained stable without any change in particle size during storage at room temperature for

235 over 8 months. The same polymerization reaction carried out without SNPs was found to be

236 too slow (conversion limited to about 70% after 6h at a temperature of 70°C) and the polymer

237 dispersion proved to be unstable, resulting in the formation of coarse lumps of polymer

238 particles swollen with monomer after several hours at 70°C. This proves that SNPs were

239 essential in achieving the successful emulsion polymerization of BMA in the absence of any

240   surfactant. We presume that the stabilization process during the formation and growth of the

241   polymer particles was the result of the attachment of the SNPs on to the polymer particles,

242   promoting what it is known as a Pickering stabilization process. Actually, as opposed to the

243   molecular surfactant, which is usually in rapid dynamic equilibrium at the oil/water interface,

244   with the shape and chemical properties of the surfactant molecules determining the

245   emulsifying behavior, in the Pickering emulsions, the oil droplet is stabilized by the reduction

246   of the bare oil-water interface due to the adsorption of the small particles. The adsorbed solid

247   particles provide an efficient steric barrier that hinders the close approach of the droplets and

248   their likely aggregation. In fact, the energetic penalty incurred by removing the adsorbed

249   particles from the interface provides the energetic barrier against coalescence. This has been

250   confirmed in this present study. Indeed, the energy required to remove the particles from the

251   interface can be estimated from Eq. (1)[19]:

252

253 $E = \gamma_{wp} R^2 (1 - \cos\theta)^2$ (1)

254

255   Where R, γ_{wp}, θ represent the particle radius, oil-water interfacial tension and three-phase

256   contact angle respectively: (R = 37 nm , θ = 43° for waxy maize, γ_{wp} = 35 mN.m^{-1})

257   This gives an energy for the SNP of 740 ($k_B T$), which is much greater than the thermal motion

258   energy of a colloidal particle $k_B T$ (8.5x10^{-21} J at 363°C : the temperature of the polymerization

259   reaction). This means that once the SNPs are attached to the polymer-water interface,

260   desorption is very difficult because the energy of desorption per particle is of the order of

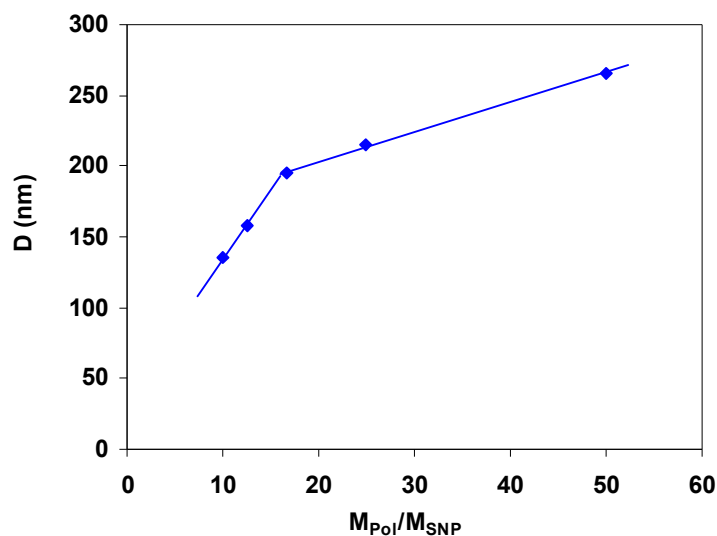261   several hundred $k_B T$.
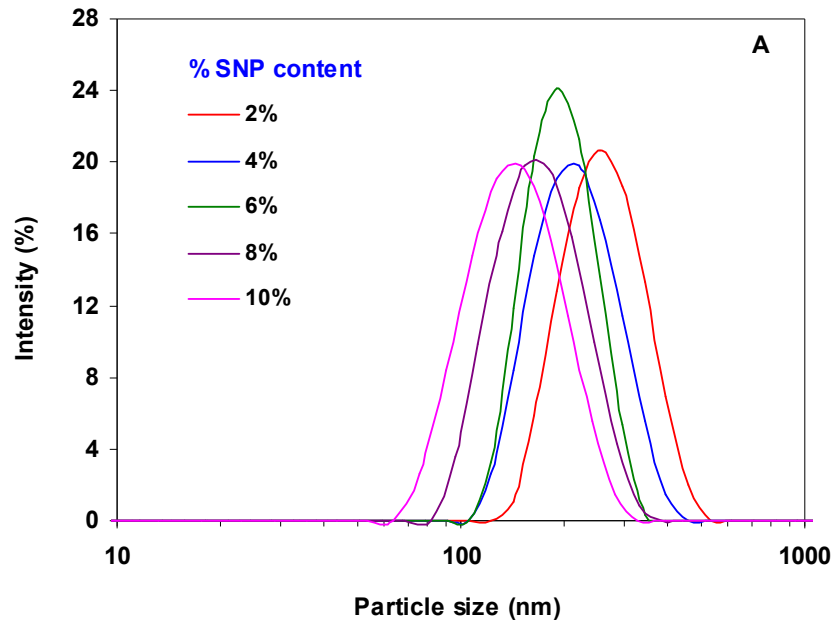
262
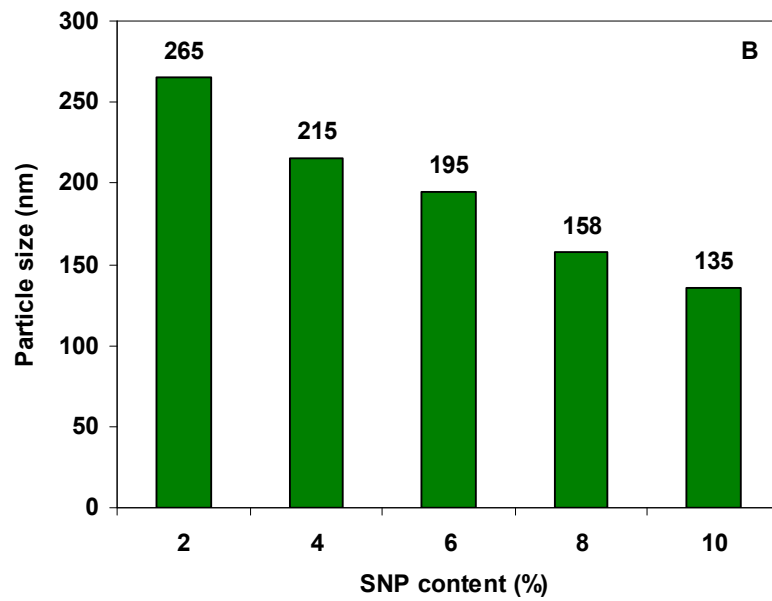
263

264

265   **Figure 4: Change in (a) particle size distribution and (b) mean particle size of the**

266   **polymer latex as a function of SNP content.**

267

14

268

Figure 5: Diameter of the polymer particle (D) vs. the polymer to SNP weight ratio

(M_{pol}/M_{SNP}) content during the Pickering emulsion polymerization.

271

272 In order to further highlight the key role of SNPs in the stabilization process, we performed a

273 series of Pickering emulsion polymerization experiments in which we varied the SNP content

274 from 2 up to 10%. As shown in Figure 4, by increasing the SNP content, a steady decrease in

275 the polymer particle size can be seen over the whole SNP loading range. The strong

276 dependence of the particle size on SNP content further emphasizes the key role of SNPs in the

277 stabilization process. Actually, in the Pickering stabilization process, the amount of stabilizing

278 solid particles controls the size of the droplets because the extent of the stabilized interfacial

279 area is proportional to the stabilizer content. If it is assumed that all available SNPs become

280 adsorbed at the polymer particle-water interface, then the interfacial area would increase

281 linearly with respect to the SNP content and the diameter of the polymer particle would be

282 proportional to the polymer to SNP weight ratio (M_{pol}/M_{SNP}) according to Eq. (2):

283 $$D = \frac{6}{\rho_{Poly}.S_{snp}} . \frac{M_{poly}}{M_{snp}}$$

(2)

284

15

285   where D is the average polymer diameter, M_{snp} and M_{pol} is the total mass of solid particles and

286   polymer particles in the system, ρ_{pol} is the polymer density and S_{snp} is the specific surface area

287   per unit mass of SNP at full coverage, i.e., the polymer particle surface covered per unit gram

288   of SNP.

289   As shown in figure 5, the linear behavior predicted by Eq. (2) was not observed over the full

290   polymer/SNP range, and two domains were noted. The first one extended from 2 to 6% SNP

291   and the second one from 6 to 10%. This behavior is put down to the involvement of two

292   modes of stabilization during the growth of the polymer particle, according to the SNP. In the

293   first domain, between 2 to 6%, electrostatic stabilization is expected to contribute to the

294   stabilization process in addition to the Pickering mode. On the other hand, over 6% SNPs, the

295   stabilization process occurs essentially via the Pickering mode. This hypothesis is supported

296   by analyzing the change in the zeta-potential of the polymer particles vs. the SNP content

297   after the complete emulsion polymerisation. The results in Figure 6 show a negative zeta-

298   potential around -20 mV as the SNP content is lower than 6%; this grows abruptly to a value

299   of around -5 mV as the SNP content exceeds 8%. Taking account the fact that the SNPs were

300   not charged (zeta-potential around -3 mV), the negative zeta-potential in the first domain

301   where the SNP content is lower than 6%, is indicative of the fact that the polymer particles

302   bear negative charges. On the other hand, with an SNP content of over 8%, the ensuing

303   polymer latex particles are not charged, as their zeta-potential is close to 0. According to the

304   colloidal stability rules, particles with a zeta-potential of around -20 mV are considered to be

305   moderately charged and should aggregate within a short period, and with a zeta-potential

306   lower than ± 5 mV, they should immediately aggregate if no physical barrier stands against

307   this irreversible process. The exceptional colloidal stability of the polymer dispersion with an

308   SNP content of more than 4%, and more specifically above 8%, where the zeta-potential is

309   close to zero, is a good indication that the stabilization process during the emulsion

310   polymerization is driven by the Pickering process. It is worth noting that the polymer

311   dispersion prepared with 8 and 10% SNPs (results not shown) did not experience any change

312   in particle size with the addition of KCl electrolyte up to a concentration of 0.1 M, which

313   further emphasizes the high colloidal stability of the polymer dispersion even at high ionic
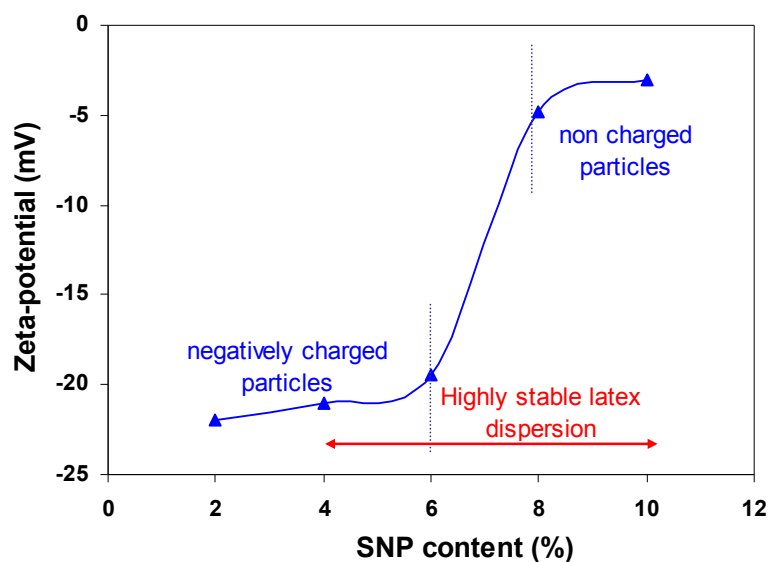
314   strength.

315

316

325   **Figure 6: Change in zeta-potential of the polymer dispersion according to SNP content**

326   **after emulsion polymerization**

327   The presence of negative charges in the domain where SNP is lower than 6% is most probably

328   due to the initiator residue (SO_4^-) accumulating on the uncovered part of the polymer

329   particles. The presence of these negative charges is likely to contribute to the stabilization

330   process as the SNP content is lower than 8%. On the other hand, above this level, the polymer

331   particles are fully covered by SNPs and their surface properties will be controlled by those of

332   the anchored solid nanoparticles.

333

17

334   The change in apparent particle size during the emulsion polymerization was monitored by

335   DLS, as shown in Figure 7. As polymerization proceeded, the particle size increased

336   continuously until the monomer droplet and the dissolved monomer were depleted.

337   Furthermore, it can also be seen that the polymerization reaction is completed within 3 h,

338   which is an acceptable kinetic with regard to the emulsion polymerization.
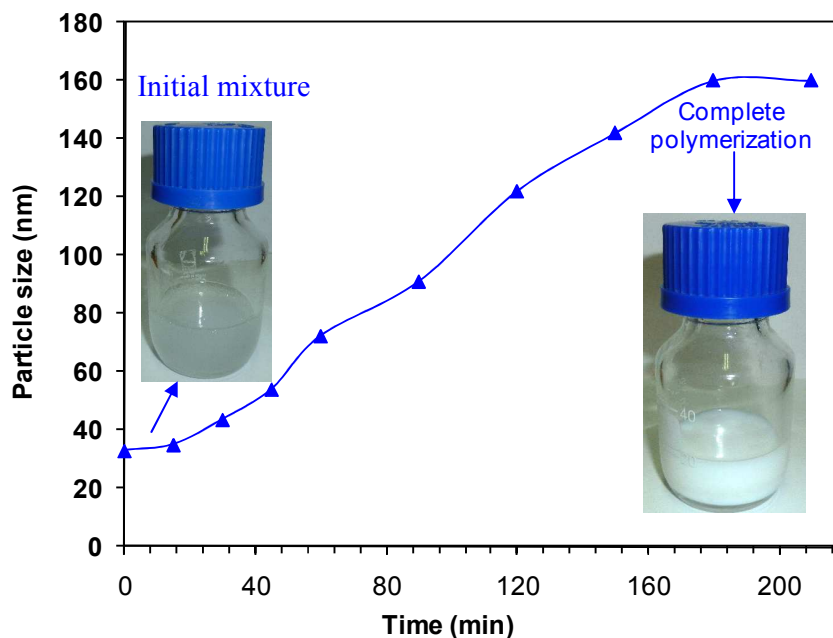
339

340   **Figure 7: Change in particle size vs. time during the course of Pickering emulsion**

341   **polymerization in the presence of 8% SNPs**

342

343   Based on the above data, the following mechanism by which the Pickering emulsion

344   polymerization of BMA takes place in the presence of SNP might be prposed upon the

345   addition of the water-soluble KPS and the temperature raising to 70°C, the decomposition of

346   the initiator produced generated free radicals free radicals in the aqueous phase, that initiated

347   the polymerization of monomer dissolved in water, forming oligomer with a terminal sulfate

348   group. When the growing macroradical reaches a critical length, it is no longer soluble in the

349   aqueous phase and precipitates to form a nucleated polymer particle. The nucleated polymer

18

350   particles are then adsorbed on the SNP and continue to grow by monomer diffusion from the

351   monomer droplet and the entry of radical into the polymer particle.. The primary particles are

352   then stabilized by SNP adsorbed onto the monomer droplet or free SNP from the aqueous

353   phase and will grow through the monomer diffusion from the droplets, which act as reservoirs

354   to supply the necessary monomer to the growing polymer particles. As the particles grow,

355   their interfacial area increases and additional solid particles are needed to ensure stabilization

356   and prevent particle aggregation. These are supplied by the direct adsorption of SNPs on the

357   grown polymer particle or result from the aggregation of the nucleated polymer particles until

358   optimum surface coverage is achieved. The polymer particles continue to grow until all the

359   monomer droplets are consumed. During this final stage, the number of particles also remains

360   constant and the polymerization rate decreases until the monomer is completely converted.

361   Two reasons might explain the preferential attachment of SNP onto the growing polymer

362   particles; first, the higher number of polymer particles compared to that of monomer droplet

363   which is the result of the difference in the size between the monomer and the nucleated

364   polymer particles (1-10μm for the former against 50-200 nm for the later), and second, the

365   higher interfacial energy of the polymer particles compared to that of the of the monomer

366   droplets.

367   ***Optical properties***

368   In nanocomposite-based material, it is extremely desirable to preserve the transparency of the

369   host matrix after the incorporation of NPs. However, even in the case of NPs measuring less

370   than 40 nm, this property is not readily achieved and a much greater drop in transparency is

371   often observed. The higher the NPs content, the greater this is.

372

373

374

375
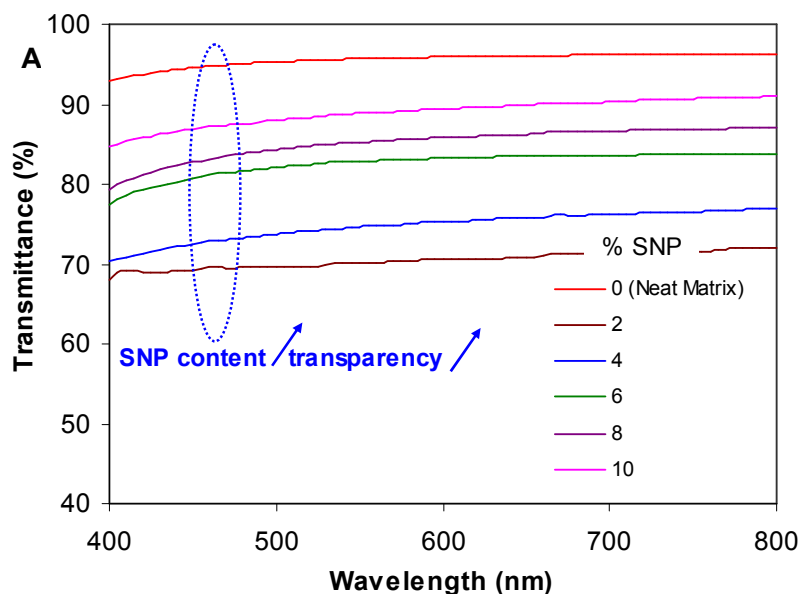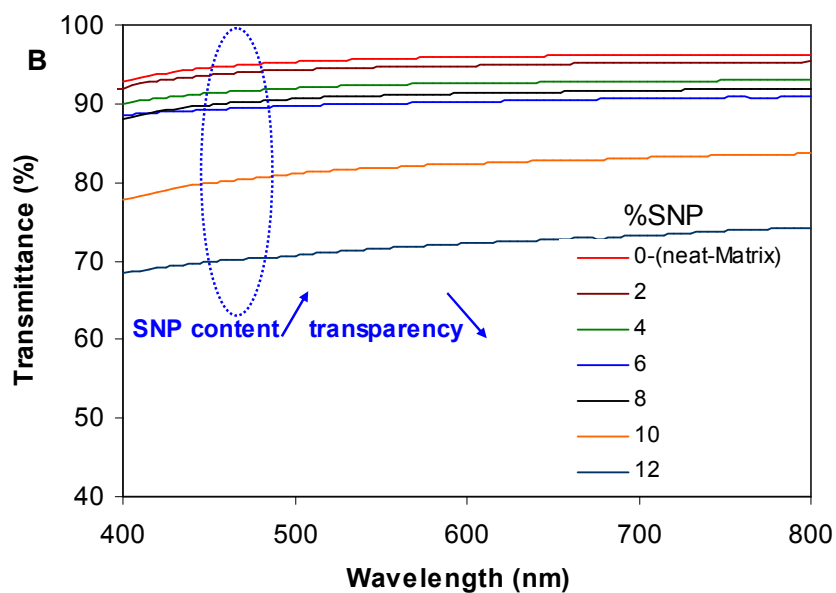
Figure 8: Transmittance spectra recorded in the visible wavelength range (thickness normalized to 200 nm) for nanocomposite film prepared via (A) the Pickering emulsion route and (B) mixing with already prepared latex dispersion

376
377
378
379

380

381   In fact, in the case of nanocomposite materials, transparency is reduced by light scattering

382   against the randomly dispersed particles. This phenomenon is dependent on both the

383   difference in refractive index between the nanoparticles and the polymer matrix, and also on

20

384   the particle size of the dispersed phase. In general, 50 nm is the upper limit for nanoparticle

385   diameter to avoid any loss in the intensity of transmitted light due to light scattering. At

386   present, due to the mismatch between the refractive index (RI) of starch (1.58)[20] and the host

387   matrix (1.48)[21] and the low particle size of the SNPs, the critical factor controlling the

388   transparency of the nanocomposites is dispersion/agglomeration of nanoparticles within the

389   host polymer matrix.

390   The optical transparency of the SNP-PBMA nanocomposite films was assessed using UV–vis

391   in the visible wavelength range of 400–800 nm (Figure 8). For the sake of comparison, the

392   nanocomposite films were prepared either via the *in situ* method using the dispersion prepared

393   through Pickering emulsion polymerisation, or through an *ex-situ* approach by mixing SNP

394   suspension with already prepared PBMA dispersion. To avoid the effect of a variation in film

395   thickness, the film transmittance was normalized to a 200 μm-thickness using the Beer–

396   Lambert law. The neat PBMA matrix was an optically transparent sheet with light

397   transmittance above 90% in the visible light wavelength range (400–800 nm). The change in

398   film transmittance with nanofiller content differs according to the preparation route. Using the

399   *in-situ* Pickering approach, the change in transmittance according to SNP content displays a

400   particular type of behavior; at 2 and 4% SNP, a meaningful drop in transmittance from about

401   95% for the neat matrix to about 70% for the nanocomposite. However, as the SNP content

402   increases, an upward shift in transmittance is observed; this is indicative of an improvement

403   in the transparency as the nanofiller loading increases. At 10% SNP content, the film

404   transmittance is close to that of the neat matrix. This indicates that, above 8% SNP, the

405   presence of the nanoparticles did not affect the high transparency of the PBMA film. In

406   contrast, when the nanocomposite films are prepared via the *ex-situ* mixing process, the

407   transmittance is maintained up to a content of 6% SNP and appreciably decreases over 8%

408   SNP, which is probably the result of aggregation or clustering of the SNPs, as their content

409   exceeds a critical threshold. This did not seem to be the case when the film was prepared via

410   the *in-situ* Pickering approach, and good dispersion of the SNPs was ensured by this method.

411   It is likely that the efficient and irreversible binding of SNPs were on to the polymer particles

412   during Pickering emulsion polymerization immobilized the NPs and accordingly prevented

413   their likelyhood aggregation during the film-formation process.

414   However, as the SNPs content is lower than 8%, the film transmittance of the film from ex-

415   situ approach is higher than that of the in-situ route. The relatively high particle size of the

416   polymer dispersion as SNPs were lower than 8% might hinder the film-formation process and

417   reduce the polymer particles coalescence. This led to surface roughness that contributed to

418   reduce the transmittance via light diffusion.

419   **Reinforcing effect**

420

421   Polysaccharide based nanofiller arouse much interst because of their huge reinforcing

422   potential when incorporated into a ductile polymer matrix. However, the reinforcing potential

423   of the nanofiller is strongly affected by the dispersion degree of nanoparticles and their

424   homogeneity within the polymer matrix. Accordingly, the processing route of the

425   nanocomposite is a key step that determines the reinforcing effectiveness of the nanofiller.

426   This is particularly the case for polysaccharide based nanoparticles, where their inherent

427   polarity and hydrogen-bonding tendency complicates homogeneous dispersion in a

428   hydrophobic polymer matrix. This explains why the most common route for the processing of

429   polysaccharide nanoparticle composites relies on the mixing of an aqueous suspension of

430   polysaccharide NPs with a waterborne polymer, followed by solvent casting and water

431   evaporation. Evidently this approach is time-consuming and limits their commercial potential,

432   despite their well-recognized exceptional reinforcing potential.

433
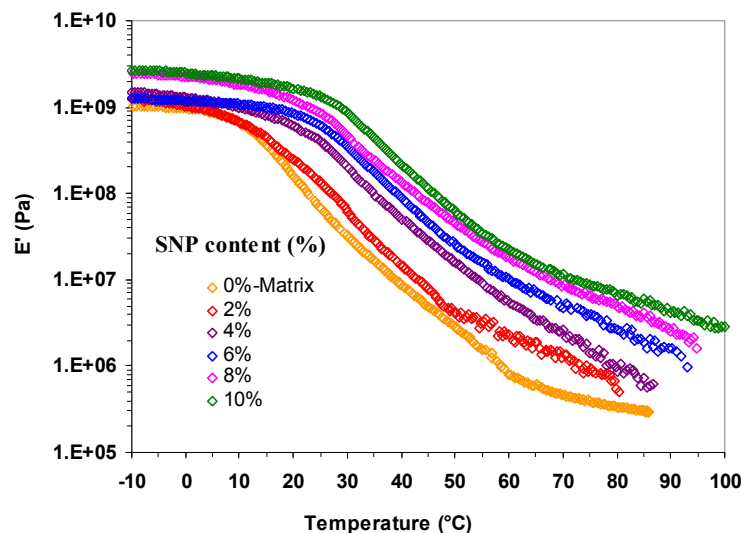
Figure 9: Storage tensile modulus, E', versus temperature at 1 Hz for nanocomposites film obtained from Pickering emulsion polymerization.

436
437
438
439   The reinforcing effectiveness of SNPs was investigated by DMA carried out on

440   nanocomposite films prepared by solvent casting of the nanocomposite dispersion prepared

441   via Pickering emulsion polymerization. The temperature dependence of the storage tensile

442   modulus, E' as a function of temperature at 1Hz for nanocomposite films with different SNP

443   contents is shown in Figure 9. Two behaviors are observed; below the glass transition

444   temperature, no significant variation in the storage modulus is detected upon the incorporation

445   of SNPs. On the other hand, above the glass transition the storage modulus is more sensitive

446   to the presence of the nanofiller and increased significantly with SNP addition, in line with

447   the well-known reinforcing effect of nanobased polysaccharide nanoparticles.[22] This means

448   that SNPs are most effective in restricting the mobility of the polymers chains above Tg.

449   To further highlight the stiffening effect imparted by the addition of SNPs the evolution of the

450   relative modulus $E_r = \dfrac{E_c}{E_{mat}}$ (with E_c and E_{mat} the storage modulus of the nanocomposite and

451   unfilled matrix respectively measured in the rubbery region taken here at 70°C) versus the

452   SNP content was drawn for the nanocomposite films prepared via Pickering emulsion

453   polymerization (Figure 10). For sake of comparison, data collected from literature for

454   nanocomposite prepared from starch nanocrystals (SNC) and latex polymer via a mixing route

455   was also shown. Even though, SNPs were not prepared via the same approach than that used

456   for SNC, the enhancement in the stiffness brought by the presence of SNPs was higher than

457   that imparted by SNC at the same loading. For instance, at 10 wt% SNPs, the modulus is 23

458   times higher than the modules of the neat matrix when Pickering emulsion polymerization

459   was adopted, while the increment is about 11-14 fold that of the neat matrix modules when

460   *the two-pots* mixing mode was used to prepare the nanocomposite film. This higher

461   reinforcing potential is a likely the result of the good dispersion of the SNPs within the

462   polymer matrix after film-formation process.

463
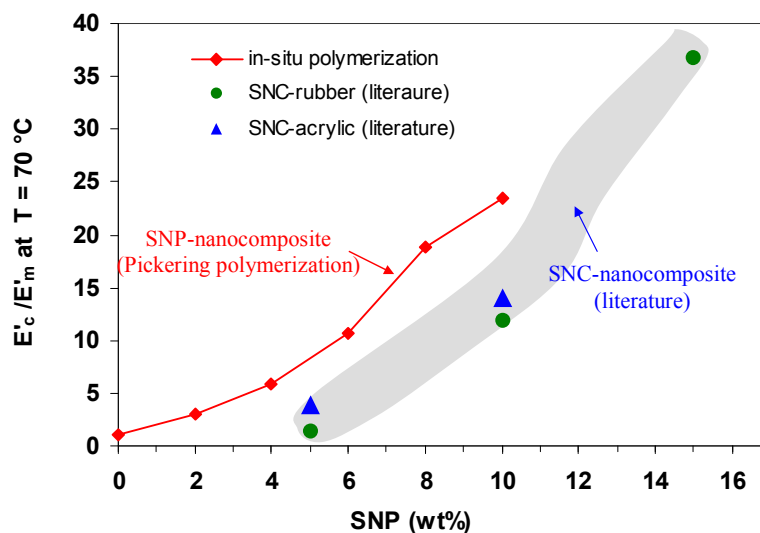
475   **Figure 10**: Relative storage modulus $E_r = \dfrac{E_c}{E_{mat}}$ versus SNP content at 70 °C for

476   nanocomposite films prepared via Pickering emulsion polymerization. Data for starch

477   nanocrystals (SNC) were extracted from literature[6],[23].

478

479

480

481   *Morphology of the polymer particles*

482
483   As shown in Figure 11, nearly spherical particles with a uniform size and raspberry-like

484   morphology could be seen. The size of the polymer particles was around 145 nm, which is in

485   agreement with the DLS data. No free SNPs were visible on the analyzed surface, which

486   might be a confirmation that all the SNPs were attached onto the polymer particles. The

487   raspberry-like morphology, along with the imperfect spherical shape, indicate that the surface

488   of the polymer particles is rough and is surrounded by densely packed nanosized SNPs,

489   confirming the role of SNPs as a stabilizer. The apparent connection between the polymer

490   particles observed during FE-SEM is probably due to their interwinding a result of the high-

491   voltage electron beam causing local heating.. This typical morphology may be attributed to

492   the mechanistic aspect of the emulsion polymerization in the presence of SNPs. As previously

493   proposed, once the nucleated particle is formed and its size increases, partial aggregation

494   among the nucleated particles stabilized by SNPs might take place to ensure enough surface

495   coverage by the SNP particles. This aggregation behavior may lead to the polymer particle

496   surface observed.
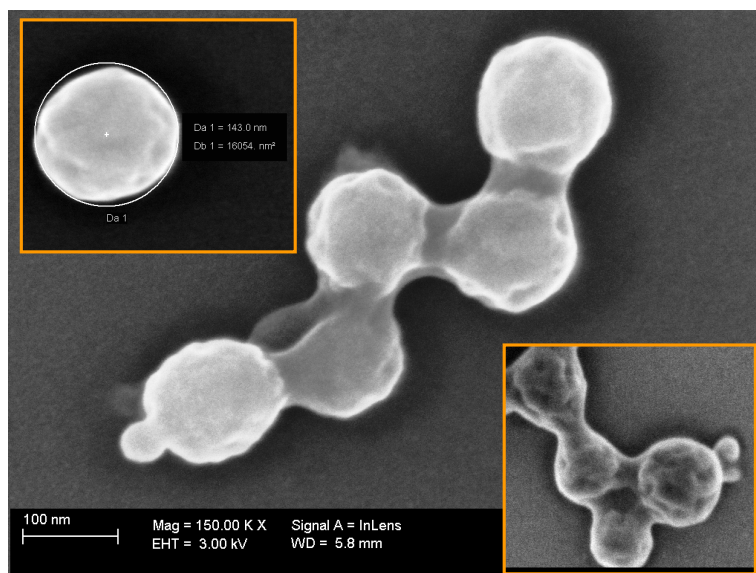
497

498   **Figure 11 : FE-SEM micrographs of freeze-dried poly(butyl methacrylate) dispersion**
499   **stabilized with 8 wt% SNP from waxy maize.**

500   **Conclusions**

501   To summarize, an easy and effective method for surfactant-free emulsion polymerization of

502   methacrylate monomer was reported, using SNPs as a Pickering stabilizer. The SNPs were

503   prepared from waxy maize using the purely physical method of high-intensity ultrasonication

504   without any chemical additives. The SNP suspensions, with a particle size of around 40 nm,

505   were used as prepared without any additional purification.

506   Pickering emulsion polymerization was easy to implement and involved mixing the monomer

507   with the SNP suspension containing the persulfate initiator, and keeping the mixture stirred

508   magnetically at 70°C for 3h. A polymer dispersion, free from any coagulum, stable for more

509   than six months, and with a particle size ranging from 250 to 150 nm, was obtained without

510   the need for additional surfactant or any non-aqueous co-solvent. It was shown that the SNP

511   content plays a key role in the stabilization process and determines the polymer particle size.

512   After the film-formation process at room temperature, the nanocomposites formed displayed

513   higher optical transparency than could be obtained by blending the polymer emulsion with an

514   SNP suspension, showing that the present approach led to a highly transparent nanocomposite

515   based on SNPs and a film-forming methacrylate monomer.

516   Overall, the present procedure demonstrates a green chemistry approach for the preparation of

517   nanocomposite dispersions based on SNPs, giving rise to high optical transparency after the

518   film-formation process. Moreover, this approach may be applicable to a wide variety of

519   vinylic and acrylic monomers, which expands its potential application to a wide range of uses

520   such as adhesives, coatings, nanocomposites and the like.

525 **References**

[1] S. Kalia, S. Boufi, A, Celli, S, Kango. Colloid. Polym. Sci., 292 (2014) 5-31.

[2] R. Jayakumar, M. Prabaharan, S.V. Nair, H. Tamura . Biotechnology Advances, 28 (2010) 142.

[3] D, Le Corre, J. Bras, A. Dufresne, Biomacromolecules, 11 (2010) 1139.

[4] D. Le Corre, E. Vahanian, A. Dufresne, J. Bras. Biomacromolecules 13 (2012) 132.

[5] J.L. Putaux, S. Molina-Boisseau, T. Momaur, A. Dufresne, A., Biomacromolecules, 4 (2003) 1198.

[6] H. Angellier, S. Molina-Boisseau,L. Lebrun, A. Dufresne., Macromolecules, 38 (2005) 3783.

[7] S. Bel Haaj, A. Magnin, C. Pétrier, S. Boufi, Carbohydrate Polymers**, 92 (**2013**)** 1625.

[8] D. S. Le Corre, J. Bras, A. Dufresne, Macromol. Mater. Eng., 297 (2012) 969.

[9] R.F.A. Teixeira, H.S. McKenzie, A.A. Boyd, S.A. Bon. Macromolecules, 44 (2011) 7415.

[10] Y. Chevalier, M.A Bolzinger. Colloid Surface A, 439 (2013) 23.

[11] L.N Butler, C.M. Fellows, R.G. Gilbert, Prog. Org. Coat. 53 (2005) 112.

[12] P.A. Kralchevsky, I.B. Ivanov, K.P. Ananthapadmanabhan, A. Lips, Langmuir, 21 (2005) 50.

[13] M. Andresen, P. Stenius, J. Dispersion Sci. Technol. 28 (2007) 837.

[14] I. Kalashnikova, H. Bizot, B. Cathala, I. Capron, Langmuir, 27 (2011) 7471.

[15] C. Li, P. Sun, C. Yang, Starch/Stärke, 64 (2012) 497.

[16] S. BelHaaj, A. B. Mabrouk, W. Thielemans, S. Boufi, Soft Matter, 9 (2013) 1975.

[17] A. B. Mabrouk, M. R. Vilar, A. Magnin, M. N. Belgacem, S. Boufi, J. Coll. Inter. Sci, 363 (2011) 136.

[18] L. A. Fielding, J. Tonnar, S. P. Armes, Langmuir, 27 (2011) 11144.

[19 S. Levine, B. D. Bowen and S. J. Partridge, Colloids Surf., 38 (1989) 343.

[20] V. Landry, A. Alemdar, P. Blanchet. Forest Product Journal, 61 (2011) 112.

[21] www.acrylite-polymers.com

[22] Dufresne, A. Molecules 15 (2010) 4111-4128.

[23] H. Angellier, J.L. Puraux, S.M.Boisseau, D.Dupeyre, A. Dufresne, Macromol. Symp. 221 (2005) 95-104